Cell Reports, Volume *37*

Supplemental information

Autotaxin impedes anti-tumor immunity by suppressing chemotaxis and tumor infiltration of $CD8^+$ T cells

Elisa Matas-Rico, Elselien Frijlink, Irene van der Haar Àvila, Apostolos Menegakis, Maaike van Zon, Andrew J. Morris, Jan Koster, Fernando Salgado-Polo, Sander de Kivit, Telma Lança, Antonio Mazzocca, Zoë Johnson, John Haanen, Ton N. Schumacher, Anastassis Perrakis, Inge Verbrugge, Joost H. van den Berg, Jannie Borst, and Wouter H. Moolenaar

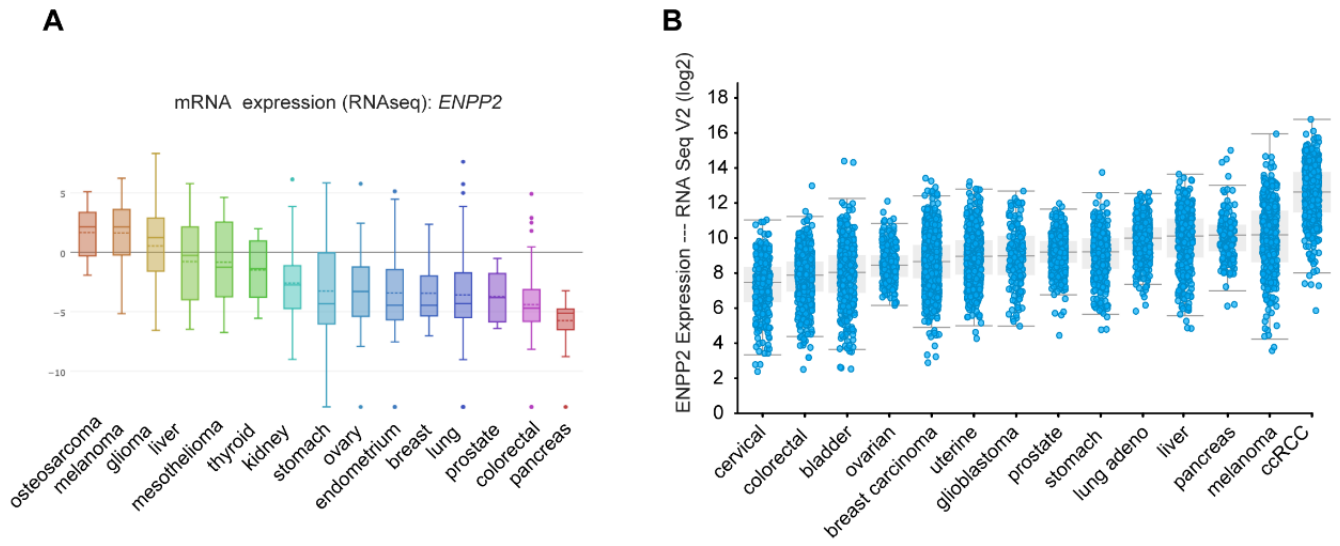

Figure S1. ATX mRNA expression in cancer cell lines and solid tumors. Related to Figures 2 and 7.
(A) *ENPP2* expression in the indicated cell lines ranked according to median values. Note high *ENPP2* expression in melanoma cell lines (n=61). RNAseq expression data were retrieved from the Cancer Cell Line Encyclopedia (CCLE; https://portals.broadinstitute.org/ccle).
(B) Pan-cancer analysis of *ENPP2* expression in the indicated solid tumors ranked according to median values (ccRCC, clear cell renal cell carcinoma). RNAseq v2 mRNA expression data were retrieved from the TCGA database (www.cbioportal.org). Note that *ENNP2* expression in cancer cell lines poorly correlates with that in the corresponding tumors, which is attributed to the presence of ATX-expressing stromal cells.

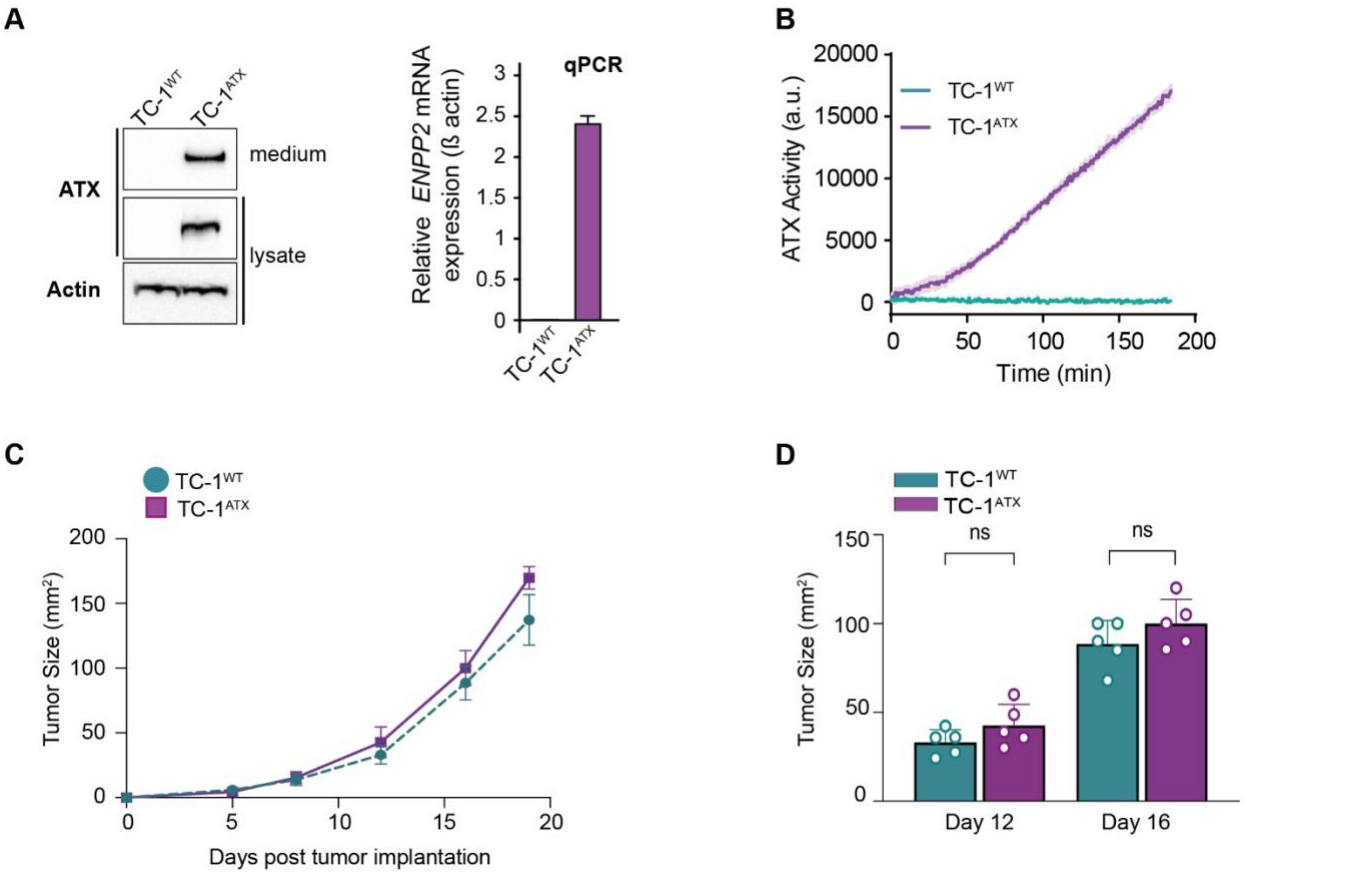

Figure S2. Characteristics of wild-type and ATX-expressing TC-1 tumors. Related to Figures 5 and 6.
(A) (Left) immunoblot analysis of ATX protein expression in wild-type (TC-1^{WT}) and ATX-expressing (TC-1^{ATX}) tumor cells. Actin was used as loading control. (Right) ATX mRNA expression (relative to Cyclophilin) in TC-1^{WT} and TC-1^{ATX} cells as analyzed by qPCR.
(B) Secreted ATX (lysoPLD) activity in supernatants from TC-1^{WT} and TC-1^{ATX} cells, as measured by choline release from added LPC(18:1) over time. See Methods for details.
(C) TC-1^{WT} and TC-1^{ATX} tumor growth expressed as mean size in non-vaccinated mice (n=5).
(D) Average tumor size in the same mice as in (**C**) on days 12 and 16 after *s.c.* tumor cell implantation. Data is depicted as mean ± SD; ns: not significant (Mann-Whitney U test).

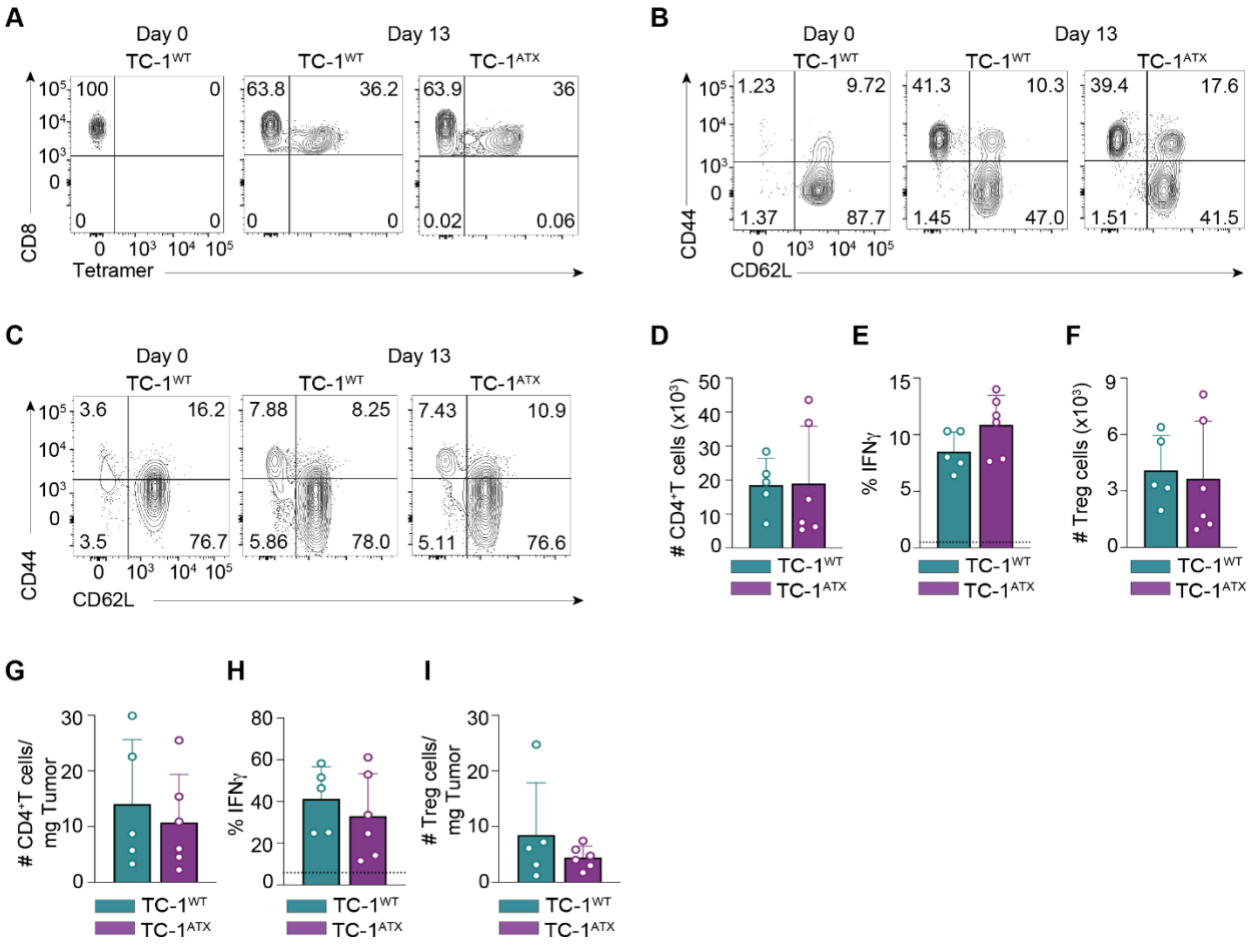

Figure S3. Enforced ATX expression in tumor cells does not affect the CD4⁺ T-cell response to vaccination. Related to Figures 5 and 6.

(A-C) Primary data belonging to **Figure 5**. Representative flow cytometry plots depicting H-2D^b/E7$_{49–57}$ Tet$^+$ cells **(A)** and CD44$^+$CD62L$^-$ effector phenotype cells among total CD8$^+$ T cells **(B)** and total CD4$^+$ T cells **(C)** in blood from TC-1^{WT} (n = 6) and TC-1^{ATX} (n = 5) tumor-bearing mice at day 13 post vaccination. Data at day 0 are from non-vaccinated TC-1^{WT} tumor-bearing mice.

(D-I) CD4$^+$ T cell populations as analyzed by flow cytometry in spleen (**D-F**) and tumors (**G-I**) of TC-1^{WT} (n = 5) and TC-1^{ATX} (n = 6) tumor-bearing mice at day 18 after tumor implantation.

(D) Absolute number (#) of FOXP3$^-$ CD4$^+$ conventional T cells (Tconv) in spleen.

(E) Frequency of IFN$_\gamma^+$ cells among conventional CD4$^+$ T cells in spleen. IFN$_\gamma$ was measured as outlined in **Figure 5**.

(F) Absolute number (#) of FOXP3$^+$ CD4$^+$ T cells (Tregs) in spleen.

(G) Absolute number (#) of CD4$^+$ Tconv cells per mg tumor tissue, found in TC-1^{WT} and TC-1^{ATX} tumor-bearing mice.

(H) Frequency of IFN$_\gamma^+$ cells within CD4$^+$ Tconv cells in the tumors. IFN$_\gamma$ was measured as outlined in Figure 5.

(I) Absolute number (#) of CD4$^+$ Tregs in TC-1^{WT} and TC-1^{ATX} tumors.

(D-I) Data are depicted as mean ± SD; no significance for all cell populations analyzed (Mann- Whitney U test). Data are from one experiment representative of two experiments.

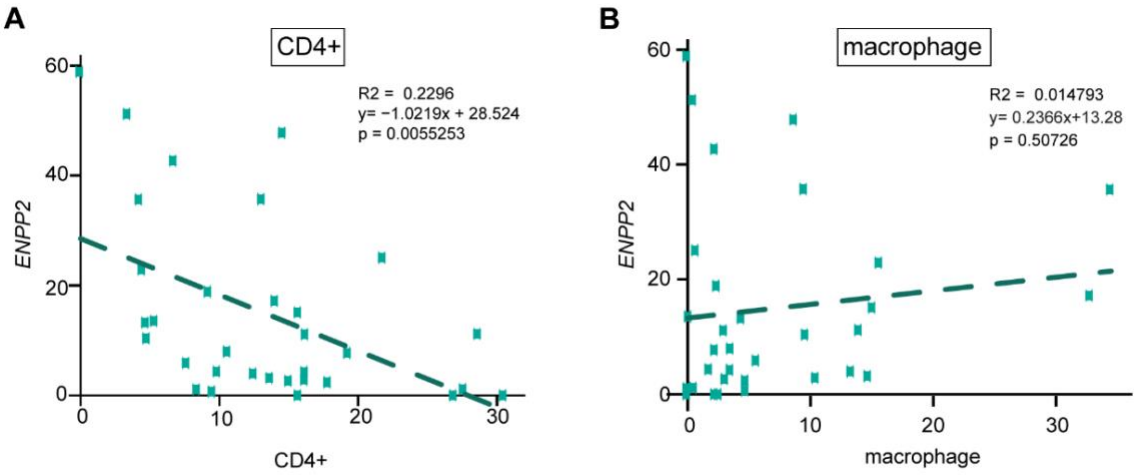

Figure S4. *ENPP2* expression and accumulation of CD4⁺ T cells (A) and macrophages (B) in melanoma tumors (n=32). Related to Figure 7.

Pearson's correlation between the percentage of inferred *ENPP2*-expressing cells and CD4⁺ T cells versus macrophages as indicated. For details see text and **Figure 7**.